中南大學
CENTRAL SOUTH UNIVERSITY

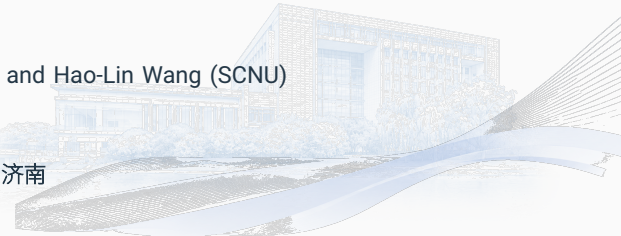
Nucleon Energy Correlators as a Probe of Light-Quark Dipole Operators at the EIC

Yingsheng Huang
Central South University

In collaboration with Xuan-Bo Tong (Jyväskylä) and Hao-Lin Wang (SCNU)

PRL 136 (2026), 131902

2026.10.17 · 第六届量子场论及其应用研讨会 · 山东济南



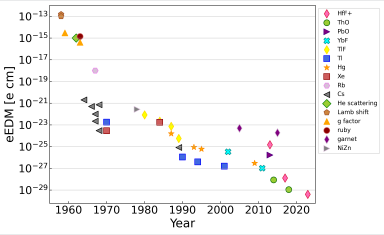
Dipole Moments in Search for BSM

Dipole moments: stringent SM tests and sensitive BSM probes.

Electron electric dipole moment

d_e **(Electron EDM)**

- $|d_e| < 4.1 \times 10^{-30} \mathrm{e} \cdot \mathrm{cm}$ (JILA).
- Constraints on BSM at $\Lambda \sim 100$ TeV.



arXiv: 2505.22281

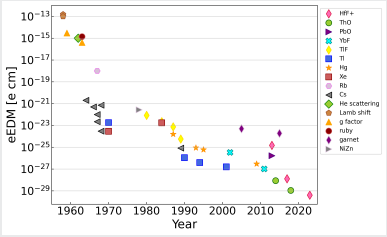
Dipole Moments in Search for BSM

Dipole moments: stringent SM tests and sensitive BSM probes.

Electron electric dipole moment

d_e (Electron EDM)

- $|d_e| < 4.1 \times 10^{-30} \mathrm{e} \cdot \mathrm{cm}$ (JILA).
- Constraints on BSM at $\Lambda \sim 100$ TeV.

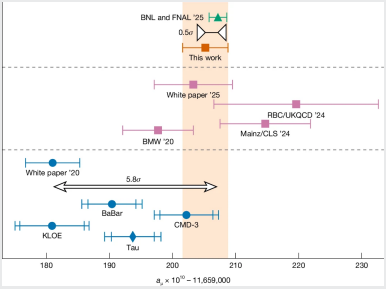


arXiv: 2505.22281

Lepton $g-2$ (magnetic dipole moments)

Muon $g-2$ (a_μ)

- FNAL '23 (190 ppb): $\sim 5\sigma$ tension.
- WP25: Tension eased (Lattice/CMD-3 HVP).



*Nature **653**, 373 (2026)*

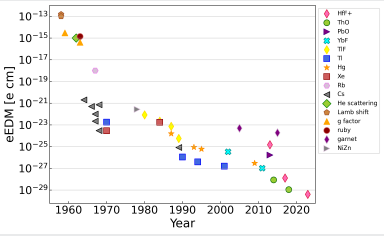
Dipole Moments in Search for BSM

Dipole moments: stringent SM tests and sensitive BSM probes.

Electron electric dipole moment

d_e (Electron EDM)

- $|d_e| < 4.1 \times 10^{-30} \mathrm{e} \cdot \mathrm{cm}$ (JILA).
- Constraints on BSM at $\Lambda \sim 100$ TeV.



arXiv: 2505.22281

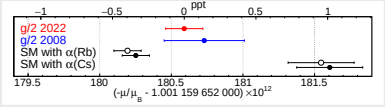
Lepton $g-2$ (magnetic dipole moments)

Muon $g-2$ (a_μ)

- FNAL '23 (190 ppb): $\sim 5\sigma$ tension.
- WP25: Tension eased (Lattice/CMD-3 HVP).

Electron $g-2$ (a_e)

- Gabrielse '23 (0.13 ppt): Tension between α determined by Cs and Rb experiments.



*PRL **130**, 071801 (2023)*

The Light Quark Sector: Current Status

Lepton dipoles have shown why dipoles are powerful on probing/eliminating BSM

$\Rightarrow$ extend the program to **light-quark dipoles**

Low-energy constraints

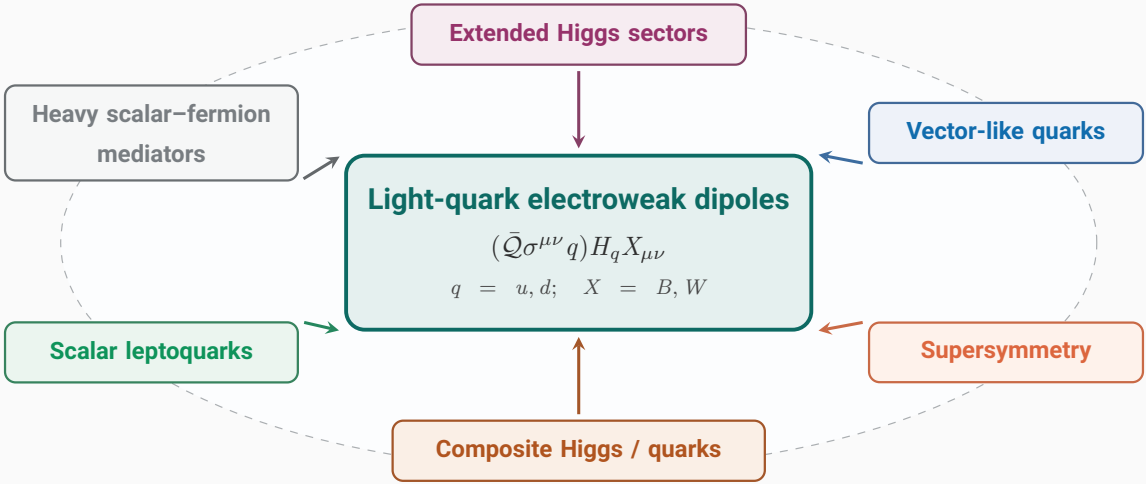
- **Neutron EDM (nEDM):** stringent bounds on light-quark EDMs.
- **Hadronic magnetic moments:** light-quark MDM bounds remain weak due to SM background.

Collider opportunity

- High-energy searches can probe *both* MDM and EDM.
- Direct access to dipole effects in a complementary kinematic regime.

Goal: precision complementary to low-energy EDM searches

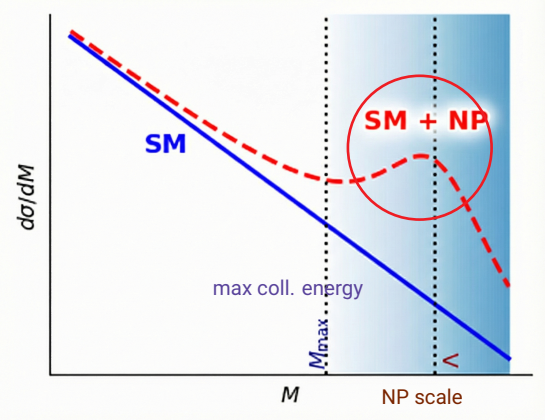
Possible UV origins of light-quark dipoles



How do we systematically search for *heavy new physics* without committing to a specific UV model?

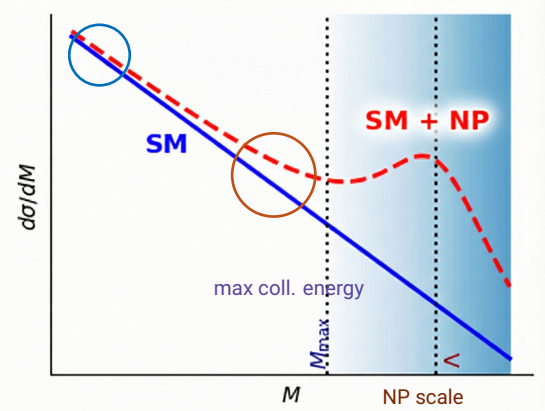


Standard Model Effective Field Theory (SMEFT)



- Heavy BSM beyond the energy reach of current collider experiments

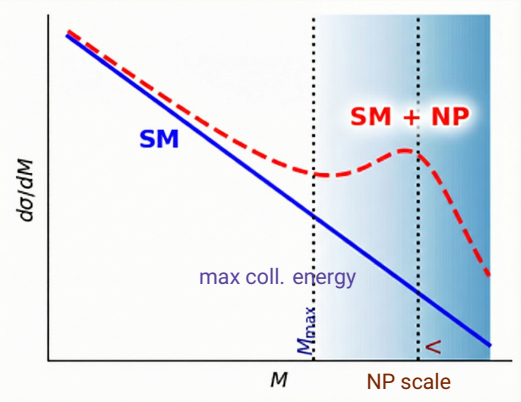
Standard Model Effective Field Theory (SMEFT)



- Heavy BSM beyond the energy reach of current collider experiments
- SMEFT provides a systematic framework to parameterize these effects below the NP scale Λ

See also Bailin Wen's talk

$$\mathcal{L}_{\text{SMEFT}} = \mathcal{L}_{\text{SM}} + \frac{1}{\Lambda^2}\sum_i C_i^{(6)}\mathcal{O}_i^{(6)} + \frac{1}{\Lambda^4}\sum_i C_i^{(8)}\mathcal{O}_i^{(8)} + \dots$$



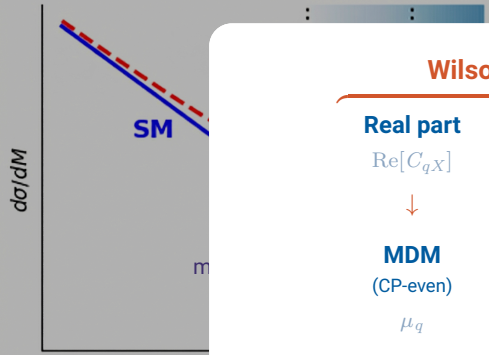
SMEFT up to dimension-6:

$$\mathcal{L}_{\rm SMEFT} = \mathcal{L}_{\rm SM} + \frac{1}{\Lambda^2}\sum_i C_i^{(6)}\mathcal{O}_i^{(6)} + \cdots$$

We focus on dimension-6 electroweak dipole operators $(+h.c.)$:

$$\mathcal{O}_{uB} = (\bar{\mathcal{Q}}\sigma^{\mu\nu}u)\tilde{H}B_{\mu\nu}$$
$$\mathcal{O}_{uW} = (\bar{\mathcal{Q}}\sigma^{\mu\nu}\tau^I u)\tilde{H}W^I_{\mu\nu}$$
$$\mathcal{O}_{dB} = (\bar{\mathcal{Q}}\sigma^{\mu\nu}d)HB_{\mu\nu}$$
$$\mathcal{O}_{dW} = (\bar{\mathcal{Q}}\sigma^{\mu\nu}\tau^I d)HW^I_{\mu\nu}$$

$\mathcal{Q}$: left-handed doublet; u, d: right-handed singlets; τ^I: SU(2) generators; $\tilde{H}_I = \epsilon_{IJ}H^*_J$.



SMEFT up to dimension-6:

$$\sum_i C_i^{(6)} \mathcal{O}_i^{(6)} + \cdots$$

weak dipole operators

$$\mathcal{Q}\, B_{\mu\nu}$$

$$)\, \tilde{H}\, W^I_{\mu\nu}$$

$$\mathcal{Q}\, B_{\mu\nu}$$

$$)\, H\, W^I_{\mu\nu}$$

Wilson coefficients

Real part	Imaginary part
$\mathrm{Re}[C_{qX}]$	$\mathrm{Im}[C_{qX}]$
↓	↓
MDM	**EDM**
(CP-even)	(CP-odd)
μ_q	d_q

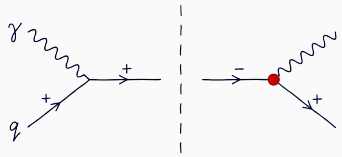
$\mathcal{Q}$: left-handed doublet; u, d: right-handed singlets; τ^I: SU(2) generators; $\tilde{H}_I = \epsilon_{IJ} H_J^*$.

However, precision collider searches face a fundamental suppression mechanism rooted in the operator structure.

Operator Structure:

- Chirality-flipping operators:

$$\mathcal{O}_{\text{dipole}} \sim \bar{\psi}_L \sigma^{\mu\nu} F_{\mu\nu} \psi_R$$



Chirality Mismatch:

- **SM:** γ^μ (odd no. of γ) $\implies$ Conserves chirality ($L \to L$).
- **Dipole:** $\sigma^{\mu\nu}$ (even no. of γ) $\implies$ Flips chirality ($L \to R$).

$\implies$ Interference term $\mathcal{M}_{\text{SM}} \times \mathcal{M}^*_{\text{dipole}} \to 0$ in massless limit

$$\text{Interference} \propto \text{Tr}[\not{k}' \gamma^\mu \not{k} \sigma^{\alpha\beta}] \xrightarrow{\text{assumed } m_q \to 0} 0 \quad \text{(Trace of odd \# of } \gamma\text{s)}$$

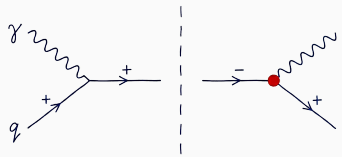
The Chirality Bottleneck at High Energy

However, precision collider searches face a fundamental suppression mechanism rooted in the operator structure.

Operator Structure:

- Chirality-flipping operators:

$$\mathcal{O}_{\text{dipole}} \sim \bar{\psi}_L \sigma^{\mu\nu} F_{\mu\nu} \psi_R$$



Chirality Mismatch:

- **SM:** γ^μ (odd no. of γ) $\implies$ Conserves chirality ($L \to L$).
- **Dipole:** $\sigma^{\mu\nu}$ (even no. of γ) $\implies$ Flips chirality ($L \to R$).

$\implies$ Interference term $\mathcal{M}_{\text{SM}} \times \mathcal{M}^*_{\text{dipole}} \to 0$ in massless limit

Consequence: only quadratic BSM sensitivity remains at leading order Boughezal et al., PRD 104, 095022 (2021)

$$\sigma \sim |\mathcal{M}_{\text{SM}}|^2 + \frac{1}{\Lambda^2}\left(\mathcal{M}_{\text{SM}} \times \mathcal{M}^*_{\text{dipole}} + \text{h.c.}\right) + \frac{1}{\Lambda^4}|\mathcal{M}_{\text{dipole}}|^2$$

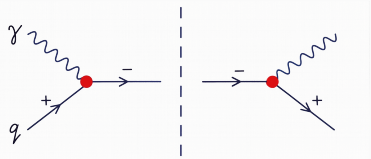
The Chirality Bottleneck at High Energy

However, precision collider searches face a fundamental suppression mechanism rooted in the operator structure.

Operator Structure:

- Chirality-flipping operators:

$$\mathcal{O}_{\text{dipole}} \sim \bar{\psi}_L \sigma^{\mu\nu} F_{\mu\nu} \psi_R$$



Chirality Mismatch:

- **SM:** γ^μ (odd no. of γ) $\implies$ Conserves chirality ($L \to L$).
- **Dipole:** $\sigma^{\mu\nu}$ (even no. of γ) $\implies$ Flips chirality ($L \to R$).

$\implies$ Interference term $\mathcal{M}_{\text{SM}} \times \mathcal{M}^*_{\text{dipole}} \to 0$ in massless limit

Consequence: only quadratic BSM sensitivity remains at leading order Boughezal et al., PRD 104, 095022 (2021)

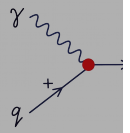
$$\sigma \sim |\mathcal{M}_{\text{SM}}|^2 + \cancel{\frac{1}{\Lambda^2}\left(\mathcal{M}_{\text{SM}} \times \mathcal{M}^*_{\text{dipole}} + \text{h.c.}\right)} + \frac{1}{\Lambda^4}|\mathcal{M}_{\text{dipole}}|^2$$

However, precision collider searches face a fundamental suppression mechanism rooted in the operator structure.

Operator Structure

- Chirality-flippi… …nserves chirality

$\mathcal{O}_{\text{dipol}}$…



$\Rightarrow$ Flips chirality

$^{*}_{\text{dipole}} \to 0$ in…

Consequence: only… …al., PRD 104, 095022 (2021)

$$\sigma \sim |\mathcal{M}_{\text{SM}}|^2 + \frac{1}{\Lambda^2}\left(\mathcal{M}_{\text{SM}} \times \mathcal{M}^{*}_{\text{dipole}} + \text{h.c.}\right) + \frac{1}{\Lambda^4}|\mathcal{M}_{\text{dipole}}|^2$$

A few issues w/ vanishing linear order

- worse sensitivity
- depends on $|C|^2$, no sensitivity to the complex phase
  $\to$ cannot constrain $\text{Re}[C]$ and $\text{Im}[C]$ individually
- same order as linear dim-8 contributions $(1/\Lambda^4)$
  $\to$ cannot ignore dim-8 contribution

The linear Λ^{-2} interference can be restored by quark transverse spin.

- **Why?** Transverse spin is a superposition of helicity states:

$$|\uparrow\rangle \propto |-\rangle + i\,|+\rangle\,.$$

- The helicity-conserving SM amplitude can therefore interfere with the helicity-flipping dipole amplitude.

Transverse-spin projector

$$u(p)\bar{u}(p) \propto \not{p}\left(1+\gamma^5 \not{S}_T\right)$$

Restores an even number of γ matrices.

The linear Λ^{-2} interference can be restored by quark transverse spin at the **EIC**.

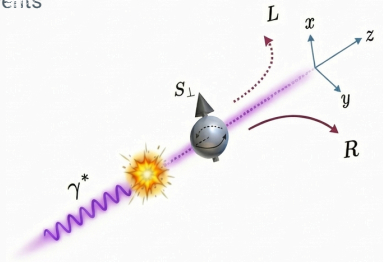
Existing Approaches:

See also Bin Yan's talk for other appl. of dihadron fragmentation

Transverse spin asymmetry @EIC

Boughezal et al. PRD 107, 075028 (2023)

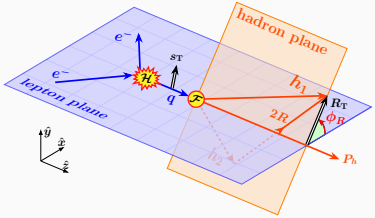
- quark transverse spin from a polarized nucleon beam
- *Limitation:* Requires polarized hadron beams, less events



Dihadron fragmentation @EIC

Wen et al., arXiv: 2408.07255

- transverse plane formed by dihadron, no need for polarized nucleon beam
- *Limitation:* requires hadron id. & tracking



The linear Λ^{-2} interference can be restored by quark transverse spin at the EIC.

Existing Approac

Transverse *on @EIC*

Boughezal

- quark transvers *adron, no need for* beam
- *Limitation:* Requ *tracking* events

Our proposal

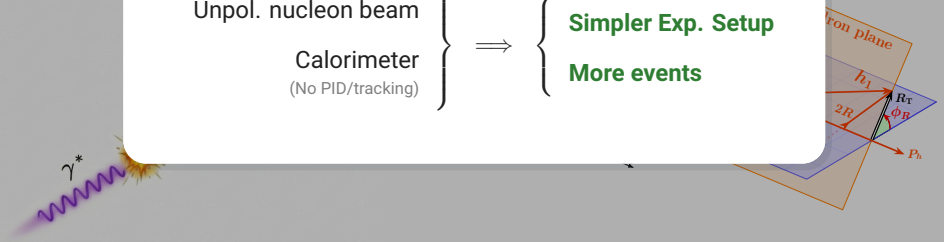
use **transversity nucleon energy correlators @EIC** to induce a transversely polarized struck quark from an unpolarized nucleon

Unpol. nucleon beam
Calorimeter (No PID/tracking)

$\Longrightarrow$

Simpler Exp. Setup

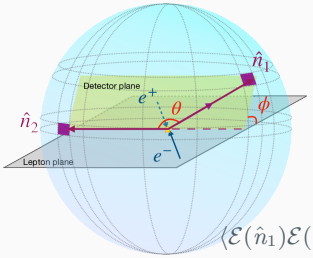
More events



ENERGY CORRELATORS (see Moult & Zhu, arXiv:2506.09119 for a review)

Energy correlators measure the energy-weighted angular correlations of particles in the detector.

See also Shu-Tao Zhang's talk

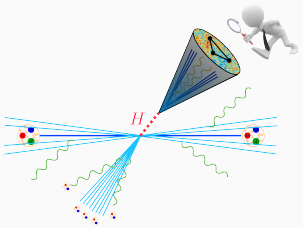


Why use them?

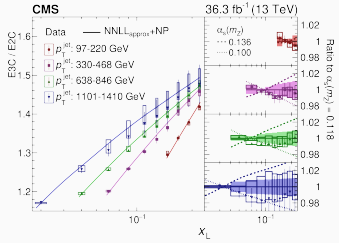
- Theoretically simple
- IRC safe → Insensitive to low-energy radiation
- No jet clustering ambiguities
- · · ·

Applications in HEP:

Jet substructure

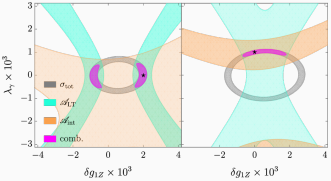


Measuring α_s



PRL 133, 071903 (2024)

BSM with TEEC

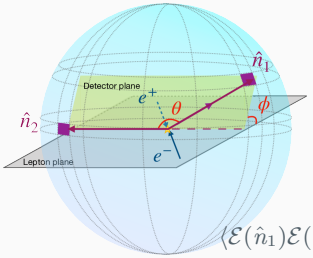


PRD 106, 114010 (2022)

ENERGY CORRELATORS (see Moult & Zhu, arXiv:2506.09119 for a review)

Energy correlators measure the energy-weighted angular correlations of particles in the detector.

See also Shu-Tao Zhang's talk



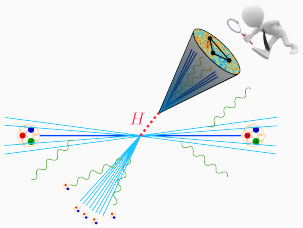
Why use them?

- Theoretically simple
- IRC safe → Insensitive to low-energy radiation
- No jet clustering ambiguities
- · · ·

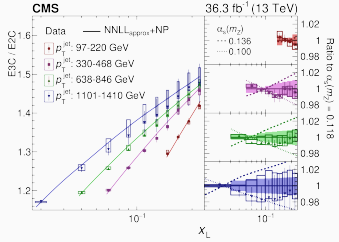
one of the few EC appl. to BSM

Applications in HEP:

Jet substructure

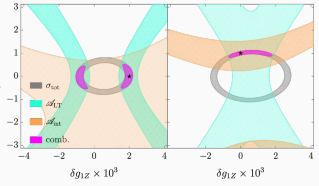


Measuring α_s



PRL 133, 071903 (2024)

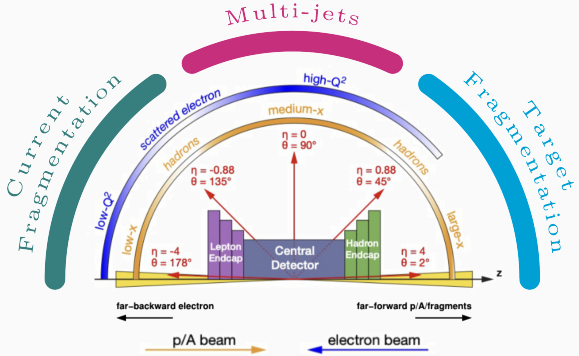
BSM with TEEC



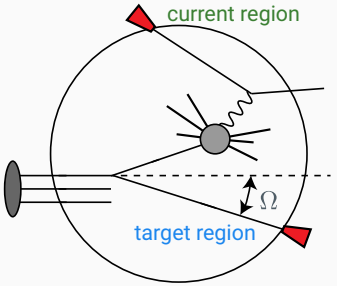
PRD 106, 114010 (2022)

Nucleon Energy Correlators (NEC) Liu & Zhu, PRL 130, 091901 (2023)

- Ordinary Energy Correlators →current fragmentation region
- **nucleon energy correlators (NECs)** are defined in the **target fragmentation region (TFR)** and probe the **initial-state nucleon remnant**.

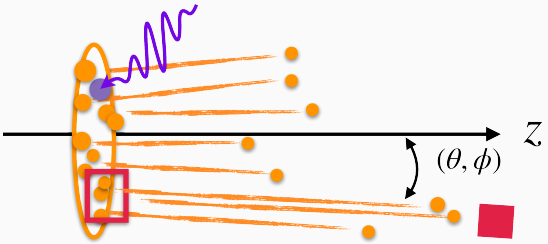


Kinematic regions @EIC. Figure from 2506.09119

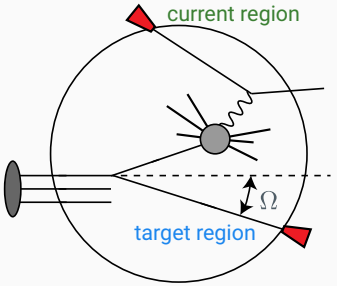


Geometry: target vs current region

- Ordinary Energy Correlators →current fragmentation region
- **nucleon energy correlators (NECs)** are defined in the **TFR** and probe the **initial-state nucleon remnant**.



NEC: probability to find a quark with long. momentum fraction x in the target, conditioned on energy flux at (θ, ϕ) in the TFR



Geometry: target vs current region

NEC: energy-weighted quark correlator

energy-flow operator

$$\mathcal{M}^{[\Gamma]}(x,\vec{\Omega}) = \int \frac{\mathrm{d}\eta^-}{4\pi} e^{-ixP^+\eta^-} \langle P|\bar{\psi}(\eta^-)\Gamma\, \mathcal{E}(\vec{\Omega})\, \psi(0)|P\rangle$$

Leading-twist decomposition of the NEC correlator:

$$\mathcal{M}_{ij}(x,\vec{\Omega}) = \frac{1}{2}\left[(\gamma^-)_{ij}\mathcal{M}^{[\gamma^+]} + (\gamma_5\gamma^-)_{ij}\mathcal{M}^{[\gamma^+\gamma_5]} - i\frac{(\sigma^-_{\alpha_\perp}\gamma_5)_{ij}}{2}\mathcal{M}^{[i\sigma^{\alpha_\perp +}\gamma_5]}\right] + \cdots$$

- **Chiral-even** unpolarized NEC f_1

  isolated from $\Gamma = \gamma^+$:

  $$f_1^q(x,\theta^2) = \mathcal{M}^{[\gamma^+]}(x,\theta,\phi)$$

- **Chiral-odd** transversity NEC h_1^t

  isolated from $\Gamma = i\sigma^{\alpha+}\gamma_5$:

  $$\epsilon_\perp^{\alpha\rho}\hat{n}_{T,\rho}\ \boldsymbol{h_1^t(x,\theta^2)} \subset \mathcal{M}^{[i\sigma^{\alpha+}\gamma_5]}$$

Leading-twist decomposition of the NEC correlator:

$$\mathcal{M}_{ij}(x,\vec{\Omega}) = \frac{1}{2}\left[(\gamma^-)_{ij}\mathcal{M}^{[\gamma^+]} + (\gamma_5\gamma^-)_{ij}\mathcal{M}^{[\gamma^+\gamma_5]} - i\frac{(\sigma^-_{\alpha_\perp}\gamma_5)_{ij}}{2}\mathcal{M}^{[i\sigma^{\alpha_\perp+}\gamma_5]}\right] + \cdots$$

- **Chiral-even** unpolarized NEC f_1

  isolated from $\Gamma = \gamma^+$:

  $$f_1^q(x,\theta^2) = \mathcal{M}^{[\gamma^+]}(x,\theta,\phi)$$

- **Chiral-odd** transversity NEC h_1^t

  isolated from $\Gamma = i\sigma^{\alpha+}\gamma_5$:

  $$\epsilon_\perp^{\alpha\rho}\hat{n}_{T,\rho}\ \boldsymbol{h_1^t(x,\theta^2)} \subset \mathcal{M}^{[i\sigma^{\alpha+}\gamma_5]}$$

  $\hat{n}_T$: transverse direction of the observed energy flux

$$i\sigma^{\alpha_\perp+}\gamma_5 = \gamma^+(\underbrace{\mathcal{Q}_+^\alpha}_{\text{Spin}\uparrow} - \underbrace{\mathcal{Q}_-^\alpha}_{\text{Spin}\downarrow})$$

$$\mathcal{Q}_\pm^\alpha = \frac{1}{2}(1 \mp \gamma^5\gamma_\perp^\alpha)$$

$\Rightarrow$ **Difference of probabilities for finding quarks polarized in two opposite directions perpendicular to the energy flux**

Leading-twist decomposition of the NEC correlator:

$$\mathcal{M}_{ij}(x,\vec{\Omega}) = \frac{1}{2}\left[(\gamma^-)_{ij}\mathcal{M}^{[\gamma^+]} + (\gamma_5\gamma^-)_{ij}\mathcal{M}^{[\gamma^+\gamma_5]} - i\frac{(\sigma^-_{\alpha_\perp}\gamma_5)_{ij}}{2}\mathcal{M}^{[i\sigma^{\alpha_\perp +}\gamma_5]}\right] + \cdots$$

- **Chiral-even** unpolarized NEC f_1

  isolated from $\Gamma = \gamma^+$:

  $$f_1^q(x,\theta^2) = \mathcal{M}^{[\gamma^+]}(x,\theta,\phi)$$

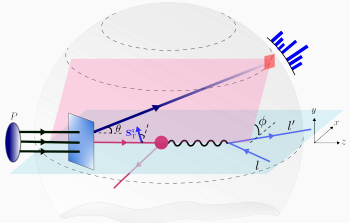
- **Chiral-odd** transversity NEC h_1^t

  isolated from $\Gamma = i\sigma^{\alpha+}\gamma_5$:

  $$\epsilon_\perp^{\alpha\rho}\hat{n}_{T,\rho}\; \boldsymbol{h_1^t(x,\theta^2)} \subset \mathcal{M}^{[i\sigma^{\alpha+}\gamma_5]}$$

$\boldsymbol{h_1^t(x,\theta^2)}$: a filter selecting the quark transverse spin in an **unpolarized nucleon**.

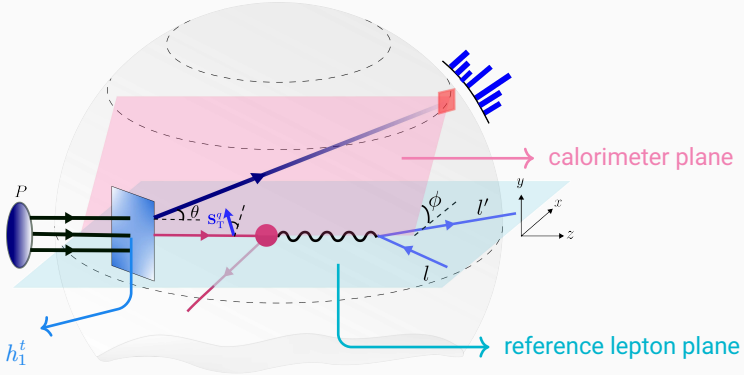
- $\Rightarrow$ **Chiral-odd nature** enables interference with *dipole operators*.
  - **Linear order** (Λ^{-2}) contribution is restored.
- h_1^t also probes the remnant energy angular distribution.



Observable: **Energy Pattern xsec.** $\Sigma(\theta, \phi)$

$$\Sigma(\theta,\phi) = \sum_{i\in X} \int \mathrm{d}\sigma^{l+p\to l'+X} \frac{E_i}{E_N} \delta(\theta^2 - \theta_i^2)\delta(\phi - \phi_i)$$

Σ: angular distribution of the total energy deposited in the calorimeters



Factorize the Energy Pattern YH, Tong & Wang, PRL 136, 131902

Factorization of the energy pattern cross section (similar to coll. factorization)

- General NEC:

Liu & Zhu, PRL 130, 091901 (2023)
Chen, Ma & Tong, JHEP 08, 227 (2024)

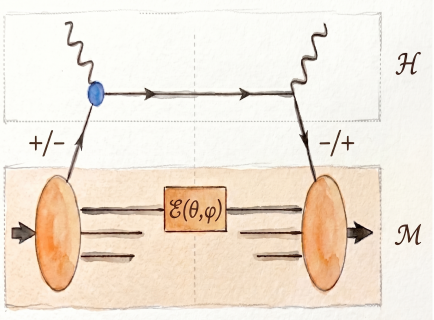
$$\frac{\mathrm{d}\Sigma(\theta,\phi)}{\mathrm{d}x_B\mathrm{d}Q^2} \propto L_{\mu\nu}\mathcal{H}^{\mu\nu}_{ji} \otimes \mathcal{M}_{ij}$$

- Transversity NEC ($\hat{n}_T = (\cos\phi, \sin\phi)$):

$$\frac{\mathrm{d}\Sigma}{\mathrm{d}x_B\mathrm{d}Q^2} \propto L_{\mu\nu}\,\mathrm{Tr}\left[\mathcal{H}^{\mu\nu}\sigma^{-\alpha}\gamma_5\right] \times \epsilon_\perp^{\alpha\beta}\hat{n}_{T\beta}\; h_1^t(x_B,\theta^2)$$

ϕ-dependence from transverse spin direction

θ-dependence



Azimuthal Modulation of the energy pattern

$$\Sigma(\theta,\phi) = \Sigma_{UU}(\theta) + \Sigma_{UU}^{\sin\phi}(\theta)\,\sin\phi + \Sigma_{UU}^{\cos\phi}(\theta)\,\cos\phi$$

SM, unpolarized NEC

Re($c_{qZ/\gamma}$), h_1^t

Im($c_{qZ/\gamma}$), h_1^t

FACTORIZE THE ENERGY PATTERN YH, Tong & Wang, PRL 136, 131902

Factorization of the **energy pattern** cross section (similar to coll. factorization)

- General NEC:

Liu & Zhu, PRL 130, 091901 (2023)
Chen, Ma & Tong, JHEP 08, 227 (2024)

$$\frac{\mathrm{d}\Sigma(\theta,\phi)}{\mathrm{d}x_B\mathrm{d}Q^2} \propto L_{\mu\nu}\mathcal{H}^{\mu\nu}_{ji} \otimes \mathcal{M}_{ij}$$

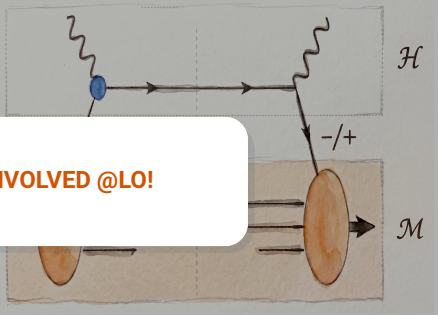
- Transversity NEC ($\hat{n}_T = (\cos\phi, \sin\phi)$):

$$\frac{\mathrm{d}\Sigma(\theta,\phi)}{\mathrm{d}x_B\mathrm{d}Q^2} \propto L_{\mu\nu}\mathcal{H}^{\mu\nu}_{ji} \otimes \mathcal{M}_{ij}$$

NO OTHER SMEFT OPERATORS INVOLVED @LO!

ϕ-dependence from transverse spin direction

θ-dependence



Azimuthal Modulation of the energy pattern

$$\Sigma(\theta,\phi) = \Sigma_{UU}(\theta) + \Sigma^{\sin\phi}_{UU}(\theta)\sin\phi + \Sigma^{\cos\phi}_{UU}(\theta)\cos\phi$$

SM, unpolarized NEC

Re($c_{qZ/\gamma}$), h_1^t

Im($c_{qZ/\gamma}$), h_1^t

General correspondence: θ-weighted moments of **NECs** $\leftrightarrow$ $k_\perp$-weighted moments of **transverse momentum dependent PDFs (TMDs)**.

Weighted NEC–TMD moments

Liu et al., arXiv:2403.08874

unpol. NEC — unpol. TMD

$$E_N \int d\theta^2 \, |\sin\theta| \, f_1(x,\theta^2) = \int \frac{d^2k_\perp}{2\pi} \, |\mathbf{k}_\perp| \, f_1(x,k_\perp^2)$$

$$E_N \int d\theta^2 \, |\sin\theta| \, h_1^t(x,\theta^2) = \int \frac{d^2k_\perp}{2\pi} \, \frac{k_\perp^2}{M} \, h_1^\perp(x,k_\perp^2)$$

YH, Tong & Wang, PRL 136, 131902

transversity NEC — Boer–Mulders TMD

Observable used below

Weight the energy pattern with $|\sin\theta|$:

$$\Sigma(\phi) = \int \mathrm{d}\theta^2 \, |\sin\theta| \, \Sigma(\theta,\phi).$$

Numerical input

- Boer–Mulders fit from **Barone et al., PRD 81, 114026 (2010).**
- The weighted moment suppresses sensitivity to local TMD-shape differences.

Azimuthal Asymmetries YH, Tong & Wang, PRL 136, 131902

Transverse spin superposition states

⌄⌄

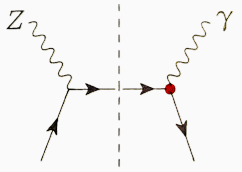
$\Sigma(\phi)$ contains a chirality-conserving contribution

⌄⌄

Extract chirality-flipping BSM effects with azimuthal asymmetries

Unpolarized beams A_{UU}

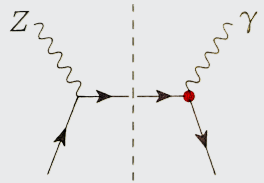
$$A^{u}_{UU} = \frac{\pi}{2}\frac{\Sigma(u>0)-\Sigma(u<0)}{\Sigma(u>0)+\Sigma(u<0)}, \qquad u = \begin{cases} \sin\phi \rightsquigarrow \mathrm{Re}\, C, \\ \cos\phi \rightsquigarrow \mathrm{Im}\, C. \end{cases}$$



γZ interference: Q^2/m_Z^2 suppression

Azimuthal Asymmetries YH, Tong & Wang, PRL 136, 131902

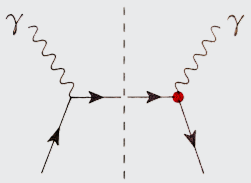
Unpolarized beams A_{UU}



$$A^{u}_{UU} = \frac{\pi}{2}\frac{\Sigma(u>0)-\Sigma(u<0)}{\Sigma(u>0)+\Sigma(u<0)}$$

Dominated by γZ interference and suppressed by Q^2/m_Z^2.

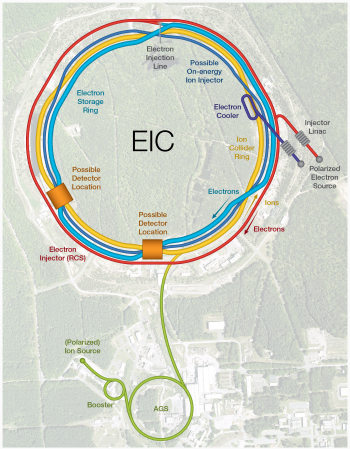
Longitudinally polarized electrons A_{LU}



The same angular partition is applied.

- Polarization activates a nonzero $\gamma\gamma$ channel.
- The leading sensitivity avoids Q^2/m_Z^2 suppression.

Application at the Electron–Ion Collider



Where to probe it?

EIC (under construction, 2034?–)

ep/eA collider at BNL

$\sqrt{s} \sim 20\text{–}140$ GeV

Moderate center-of-mass energy

$\mathcal{L}_{\text{int}} \sim 10\text{–}100\ \text{fb}^{-1}$

High luminosity

High luminosity enables precision measurements of the DIS asymmetries.

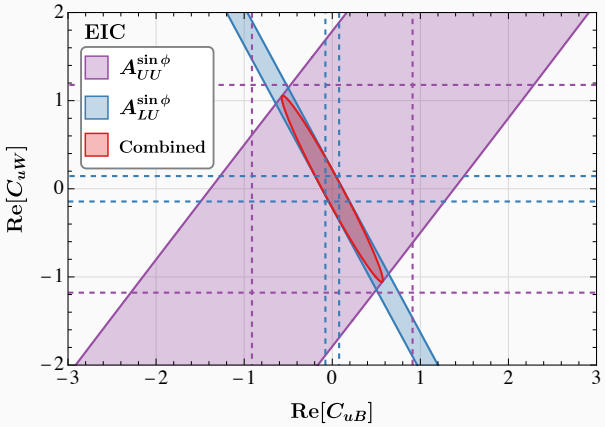
Constraints w/ EIC

- $\mathbf{A}_{\mathbf{UU}}^{\sin\phi}$: Strong correlation between C_{uW} and C_{uB}, leaving a "flat direction" unconstrained.
- $\mathbf{A}_{\mathbf{LU}}^{\sin\phi}$: Polarized electron beam
  $\Longrightarrow$ nonzero $\gamma\gamma$ interference
  $\Longrightarrow$ seemingly tighter constraints pointing at another direction.
- Single-operator constraints reach $\mathcal{O}(10^{-2})$ at $\Lambda = 1$ TeV.

The combined fit breaks the degeneracy and improves parameter resolution by orders of magnitude.

$\sqrt{s} = 105$ GeV, $\mathcal{L} = 100\,\text{fb}^{-1}$, $P_e = 70\%$

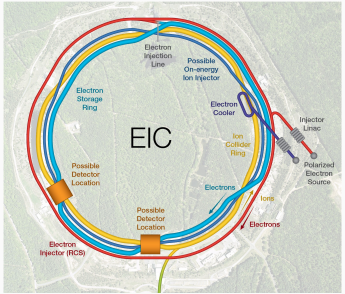
$\delta A \simeq \frac{\pi}{2\sqrt{\mathcal{E}_{\text{total}}\mathcal{L}}}$ (stat. only)



Applications at Electron–Ion Colliders

Under construction: EIC (2034–)

- First highly polarized ep/eA collider.
- $\sqrt{s} \sim 20\text{–}140\ \mathrm{GeV}$.
- High luminosity: $10\text{–}100\ \mathrm{fb}^{-1}$.



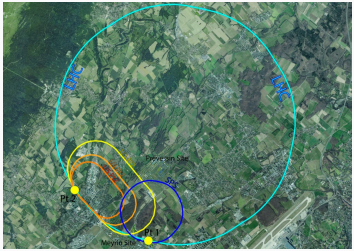
Past: HERA (1991–2007)

- DESY ep collider.
- $\sqrt{s} \simeq 318\ \mathrm{GeV}$.
- Low luminosity.
- Existing data provide constraints.



Future: LHeC (?)

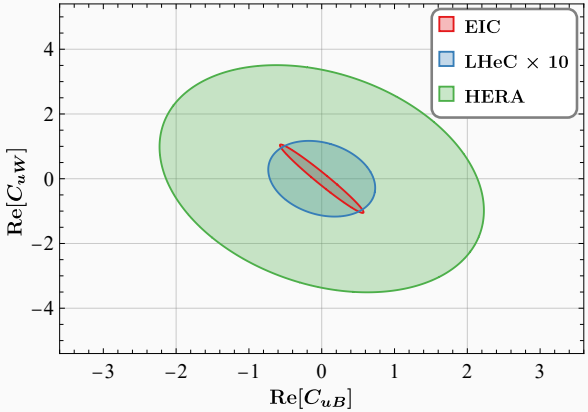
- Proposed ep collider using the LHC proton beam.
- $\sqrt{s} \sim 1.3\ \mathrm{TeV}$ (run 6).
- High energy and luminosity.
- Future uncertain.



HERA and LHeC may also constrain light-quark dipole operators.

Comparison btw. electron-ion colliders

	$\sqrt{s}$ [GeV]	$\mathcal{L}$ [fb^{-1}]	P_e
HERA	318	0.4	40%
EIC	105	100	70%
LHeC	1300	50	80%



Collider Sensitivity:

- **HERA:** High Q^2 coverage but limited by luminosity and lack of polarization.
- **EIC:** Polarization breaks γ/Z degeneracy; high $\mathcal{L}$ drives precision.
- **LHeC:** Potential to improve bounds by another order of magnitude.

Summary

The angular dist. of energy flow lets the EIC **linearly probe light-quark dipole operators**.

- **Transversity NEC** h_1^t filters transverse quark polarization from an unpolarized nucleon.
- **Linear interference** between the SM and dipole amplitudes **reappears** at $\mathcal{O}(\Lambda^{-2})$.

- $\sin\phi$ and $\cos\phi$ probe the **real (MDM)** and **imaginary (EDM)** parts, respectively.
- **No other SMEFT operators** enter at leading order.

- **No polarized nucleon beam** is required.
- **Calorimetric meas.** avoid particle id. and track reconstruction.
- EIC precision can compete with traditional BSM probes.

Nucleon energy correlators open a new avenue to **BSM searches** through **energy flow**.

Backup

We focus on dimension-6 electroweak dipole operators ($+h.c.$):

$$\mathcal{O}_{uB} = (\bar{\mathcal{Q}}\sigma^{\mu\nu}u)\tilde{H}B_{\mu\nu} \qquad \mathcal{O}_{uW} = (\bar{\mathcal{Q}}\sigma^{\mu\nu}\tau^I u)\tilde{H}\,W^I_{\mu\nu}$$
$$\mathcal{O}_{dB} = (\bar{\mathcal{Q}}\sigma^{\mu\nu}d)H\,B_{\mu\nu} \qquad \mathcal{O}_{dW} = (\bar{\mathcal{Q}}\sigma^{\mu\nu}\tau^I d)H\,W^I_{\mu\nu}$$

$\mathcal{Q}$: Left-handed doublet; u, d: Right-handed singlets, τ^I: SU(2) generators.

Effective couplings after EWSB:

$$\mathcal{L}_{\text{eff}} \supset \sum_{q=u,d} \bar{q}_L\,\sigma^{\mu\nu}\,q_R\left(c_{q\gamma}F_{\mu\nu} + c_{qZ}Z_{\mu\nu}\right) + h.c.$$

The complex coefficients ($c_{q\gamma}$, c_{qZ}) are rotations of SMEFT (C_{qB}, C_{qW}):

$$c_{q\gamma} = (v/\sqrt{2}\Lambda^2)\,(c_W\,C_{qB} \pm s_W\,C_{qW})\,,$$
$$c_{qZ} = (v/\sqrt{2}\Lambda^2)\,(-s_W\,C_{qB} \pm c_W\,C_{qW})\,,$$

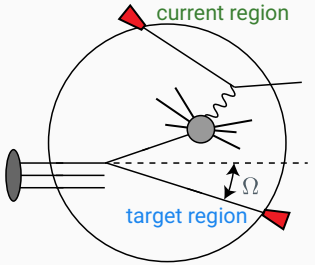
v: Higgs vev., c_W, s_W: cosine and sine of Weinberg angle θ_W.

- Unlike Energy Correlators in the Current Region, NECs are defined in the **target fragmentation region (TFR)** and probe the **initial-state nucleon remnant**.
- **Definition:** Probability of finding a quark with momentum fraction x inside the target, given energy flux at (θ, ϕ) in the TFR.

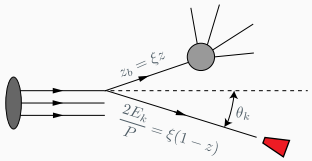
$$\mathcal{M}_{ij}(x,\theta,\phi) = \int \frac{d\eta^-}{2\pi} e^{-ixP^+\eta^-} \langle PS|\bar{\psi}_j(\eta^-) \mathcal{L}_n^\dagger(\eta^-)\mathcal{E}(\theta,\phi)\mathcal{L}_n(0)\psi_i(0)|PS\rangle \,,$$

where the *Energy Flow Operator* $\mathcal{E}$ follows

$$\mathcal{E}(\theta,\phi)|X\rangle = \sum_{i\in X} \frac{E_i}{E_N}\delta(\theta_i^2-\theta^2)\delta(\phi_i-\phi)|X\rangle$$



Geometry: target vs current region



Energy flux from target remnants measured in forward calorimeters

unpol. quark

long. quark

$$\mathcal{M}_{ij}(x,\theta,\phi,S) = \frac{1}{2}\Big[(\gamma^-)_{ij}\mathcal{M}^{[\gamma^+]} + (\gamma_5\gamma^-)_{ij}\mathcal{M}^{[\gamma^+\gamma_5]} - i\frac{g_{\alpha\beta}^{\perp}}{2}(\sigma^{\beta-}\gamma_5)_{ij}\mathcal{M}^{[i\sigma^{\alpha+}\gamma_5]}\Big] .$$

trans. quark

trans. quark

trans. proton

long. proton

$$\mathcal{M}^{[i\sigma^{\alpha+}\gamma_5]}(x,\theta,\phi,S) = S_T^{\alpha} h_1(x,\theta) + \frac{S_L \mathbf{n}_t^{\alpha}}{|\mathbf{n}_t|} h_{1L}^t(x,\theta) - \left(\frac{g_T^{\alpha\rho}}{2} + \frac{\mathbf{n}_t^{\alpha}\mathbf{n}_t^{\rho}}{|\mathbf{n}_t|^2}\right) S_{T\rho} h_{1T}^t(x,\theta) + \frac{\epsilon_{\perp}^{\alpha\rho}\mathbf{n}_{t,\rho}}{|\mathbf{n}_t|} h_1^t(x,\theta) .$$

trans. proton (pretzelosity)

unpol. proton

How does an unpolarized nucleon provide polarized quarks?

- **Decomposition:** The quark correlator $\mathcal{M}_{ij}$ contains a chiral-odd term:

$$\mathcal{M}^{[\Gamma_\perp^\alpha]} = \frac{1}{2}\mathrm{Tr}\left[(i\sigma^{\alpha_\perp +}\gamma_5)\mathcal{M}\right]$$

- **Spin Projector:** This operator projects onto transverse spin states along direction $\alpha_\perp$:

$$i\sigma^{\alpha_\perp +}\gamma_5 = \gamma^+(\underbrace{\mathcal{Q}_+^\alpha}_{\text{Spin}\uparrow} - \underbrace{\mathcal{Q}_-^\alpha}_{\text{Spin}\downarrow})$$

where $\mathcal{Q}_\pm^\alpha = \frac{1}{2}(1 \mp \gamma^5\gamma_\perp^\alpha)$ selects quarks with spin $\parallel$ or anti-$\parallel$ to the transverse vector $\alpha_\perp$.

How does an unpolarized nucleon provide polarized quarks?

- **Decomposition:** The quark correlator $\mathcal{M}_{ij}$ contains a chiral-odd term:

$$\mathcal{M}^{[\Gamma_\perp^\alpha]} = \frac{1}{2}\mathrm{Tr}\left[(i\sigma^{\alpha_\perp +}\gamma_5)\mathcal{M}\right]$$

- **Symmetry Argument:** In an unpolarized nucleon, the *only* transverse reference vector is the energy flow direction $\hat{n}_T = (\cos\phi, \sin\phi)$.
- **Form Factor:** Rotational invariance dictates the structure:

$$\mathcal{M}^{[\Gamma_\perp^\alpha]} \propto \epsilon_\perp^{\alpha\beta}\hat{n}_{T,\beta}\, h_1^t(x,\theta^2)$$

- **Mechanism:** Selecting an energy flow direction ϕ breaks rotational symmetry and ”filters” the quark bath, preferentially selecting quarks with transverse spin correlated with ϕ.

Factorization of the energy pattern cross section

- General NEC:

$$\frac{\mathrm{d}\Sigma(\theta,\phi)}{\mathrm{d}x_B\mathrm{d}Q^2} \propto \int_{x_B}^{1} \frac{\mathrm{d}x}{x} L_{\mu\nu}(l,l')\mathcal{H}^{\mu\nu}_{ji}\left(\frac{x_B}{x}\right)\delta(1-\frac{x_B}{x})\mathcal{M}_{ij}(x,\theta,\phi)$$

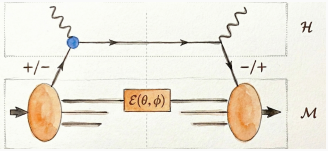
- Transversity NEC:

$$\frac{\mathrm{d}\Sigma}{\mathrm{d}x_B\mathrm{d}Q^2} \propto L_{\mu\nu}\,\mathrm{Tr}\left[\mathcal{H}^{\mu\nu} i\sigma^{-\alpha}\gamma_5\right]\epsilon_\perp^{\alpha\beta}\hat{n}_{T\beta}h_1^t(x_B,\theta^2)$$

Coupling of h_1^t with dipole-SM interference

$$\mathrm{d}\Sigma \propto \left[\mathcal{C}_1 \sin\phi + \mathcal{C}_2 \cos\phi\right] h_1^t\,(x_B,\theta^2)$$

$\mathcal{C}_1$: Re($c_{qZ/\gamma}$) $\mathcal{C}_2$: Im($c_{qZ/\gamma}$) h_1^t: transversity NEC



SM Background:

$$\frac{\mathrm{d}\Sigma_{UU}}{\mathrm{d}x_B \mathrm{d}Q^2} = \frac{2\pi\alpha_{\mathsf{em}}^2}{Q^4} \sum_q f_1^q(x_B,\theta^2)\Bigg\{ Q_q^2(y^2-2y+2) + \frac{2Q^2}{Q^2+m_Z^2}\frac{Q_q}{(c_W s_W)^2}\Big[g_A^e g_A^q (y-2)y - g_V^e g_V^q (y^2-2y+2)\Big] + \frac{1}{(c_W s_W)^4}\left(\frac{Q^2}{Q^2+m_Z^2}\right)^2 \Big[(y^2-2y+2)[(g_A^e)^2 + (g_V^e)^2][(g_A^q)^2+(g_V^q)^2] - 4y(y-2) g_A^e g_A^q g_V^e g_V^q\Big]\Bigg\}$$

SMEFT Signal (Interference):

$$\frac{\mathrm{d}\Sigma_{UU}^{\sin\phi}}{\mathrm{d}x_B \mathrm{d}Q^2} = \frac{4\pi\alpha_{\mathsf{em}}^2}{e c_W s_W}\frac{y\sqrt{1-y}}{Q(Q^2+m_Z^2)} \sum_q h_1^{t,q}(x_B,\theta^2)\Bigg\{ \Big[\frac{2-y}{y} g_A^q g_V^e + g_V^q g_A^e\Big]\frac{\mathsf{Re}[c_{q\gamma}]}{c_W s_W} - Q_q g_A^e \mathsf{Re}[c_{qZ}] + \frac{1}{(c_W s_W)^2}\frac{Q^2}{Q^2+m_Z^2}\Big[\frac{2-y}{y}[(g_A^e)^2+(g_V^e)^2] g_A^q + 2 g_A^e g_V^e g_V^q\Big]\mathsf{Re}[c_{qZ}]\Bigg\}$$

Beam and phase space

- **CM energy:** $\sqrt{s} = 105$ GeV.
- **Luminosity:** $\mathcal{L} = 100\,\text{fb}^{-1}$.
- $Q \in [10, 60]$ GeV, $\quad x \in [0.01, 0.5]$.
- Inelasticity cut: $0.1 \leq y \leq 0.9$.
- TMD moment range:

$$k_\perp^{\min} \sim E_{\min}\theta_{\min}, \qquad k_\perp^{\max} \sim Q\theta_{\max},$$

implemented as $k_\perp \in [0, 5]$ GeV.

Statistical sensitivity

$$\delta A \simeq \frac{\pi}{2\sqrt{\mathcal{E}_{\text{total}}}}, \qquad \mathcal{E}_{\text{total}} = [\Sigma(u > 0) + \Sigma(u < 0)]\mathcal{L}.$$

Limits follow from

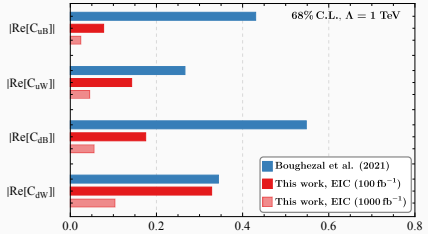
$$\chi^2 = \sum_i \left[\frac{A_{\text{th},i} - A_{\text{exp},i}}{\delta A_i}\right]^2.$$

Observables

1. $A_{UU}^{\sin\phi}$: unpolarized e^- and p.
2. $A_{LU}^{\sin\phi}$: $P_e = 70\%$ and unpolarized p.

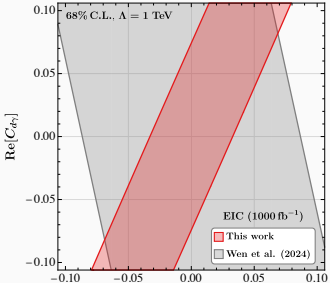
vs. LHC Drell-Yan ($pp \to Z/\gamma^* \to \ell\ell$)

- DY: Dipole effects at $\mathcal{O}(\Lambda^{-4})$ (squared) $\Longrightarrow$ weaker bounds despite higher energy.
- Contamination from other dim-6/8 operators.
- Cannot resolve complex phase.
- **NEC Advantage:** Leading $\mathcal{O}(\Lambda^{-2})$ contrib., clean separation of Re/Im.



vs. EIC Dihadron ($ep \to e(h_1h_2)X$)

- Relies on interference in dihadron fragmentation.
- Requires particle ID and tracking.
- **NEC Advantage:** Simpler inclusive calorimetric measurement; $\sim 10\times$ better sensitivity (for same lumi).



Input Dependence:

- Input: Boer-Mulders TMD $h_1^\perp$.
- Comparison of 3 fits: Barone et al. (default), Christova et al., Zhang et al.
- Result: Constraints are robust against fit choice.
- Reason: Observable sensitive to $k_\perp$-weighted moment, integrating out local shape differences.

